Journal of Power Sources 237 (2013) 291–294

Contents lists available at SciVerse ScienceDirect

Journal of Power Sources

journal homepage: www.elsevier.com/locate/jpowsour

Short communication

Facile preparation and electrochemical properties of amorphous SiO_2/C composite as anode material for lithium ion batteries

Pengpeng Lv [a], Hailei Zhao [a,b,*], Jing Wang [a], Xin Liu [a], Tianhou Zhang [a], Qing Xia [a]

[a] School of Materials Science and Engineering, University of Science and Technology Beijing, Beijing 100083, China
[b] Beijing Key Lab of New Energy Materials and Technologies, Beijing 100083, China

HIGHLIGHTS

- Amorphous SiO_2/C composite was prepared via a facile route.
- SiO_2/C electrode exhibits high specific capacity and stable cycling performance.
- SiO_2/C electrode displays excellent rate-capability.
- Amorphous SiO_2 shows higher electrochemical activity than crystalline one.

GRAPHICAL ABSTRACT

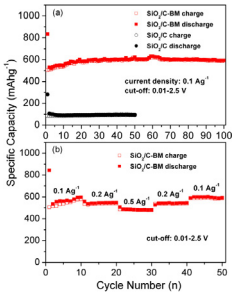

ARTICLE INFO

Article history:
Received 10 January 2013
Received in revised form
11 March 2013
Accepted 12 March 2013
Available online 21 March 2013

Keywords:
Sol–gel
Mechanical milling
Silicon oxide
Anode material
Lithium ion batteries

ABSTRACT

An amorphous SiO_2/C composite anode material is synthesized via a sol–gel route combining with mechanical milling and post heat-treatment processes. The synthesized amorphous SiO_2/C composite presents a nanostructure composing of amorphous SiO_2 cluster and coating carbon layer. The amorphous SiO_2/C electrode exhibits high reversible capacity (~600 mA h g^{-1}), stable cycling performance and excellent rate-capability. Mechanical milling causes SiO_2/C composite amorphization which makes the active material possess good electrochemical activity. The coating carbon layer can not only increase electronic conductivity, but also accommodate part of the volume expansion occurred during discharge/charge process.

1. Introduction

There is an increasing demand for rechargeable lithium-ion batteries with higher energy density and longer cycle life for applications in portable electronic devices and electric vehicles [1]. Carbonaceous material is commonly used as anode material in commercialized lithium ion batteries due to its advantages of long cycle life and low cost. However, its low lithium-storage capacity cannot satisfy the requirement on electrode materials of high energy density batteries. Various materials with higher specific capacity have been proposed as new anode candidates, such as Sn-based [2,3], Sb-based [4,5], and Si-based materials [6–9]. Among them, the Si-based materials have attracted great interest due to the significantly higher theoretical specific capacity of about 4200 mA h g^{-1} for $Li_{22}Si_5$ alloy, abundance in natural reserves, low-cost and higher safety [10]. The application of Si-based anode is

* Corresponding author. School of Materials Science and Engineering, University of Science and Technology Beijing, Beijing 100083, China. Tel./fax: +86 10 82376837.
E-mail addresses: hlzhao@ustb.edu.cn, hlzhao66@gmail.com (H. Zhao).

0378-7753/$ – see front matter © 2013 Elsevier B.V. All rights reserved.
http://dx.doi.org/10.1016/j.jpowsour.2013.03.054

hindered, however, by its poor cycling performance. Si-based electrodes suffer from the severe volume changes during Li insertion/extraction process, which easily leads to electrode cracking or pulverization, and thus severe capacity degradation. Tremendous endeavours have been made to overcome this problem by preparing nanoparticles [11], thin films [12–14] and Si-based composites [15–17], including carbon coated Si powders [18–25]. Among these works, high performance was achieved by dispersing nano Si particles in carbon matrix [18–22] or coating nano Si particles with carbon [23–25]. The carbon matrix could prevent the Si particle from aggregation during electrochemical cycling and enhance the electronic conductivity. However, the high cost of nano silicon makes the anode composite far from industrial application level.

The employment of silicon oxide material is another effective way to improve the cycling performance of silicon-based anode [26–28]. Lithium ions react with silicon oxides to produce nano-Si domains and inert Li_4SiO_4 and/or Li_2O oxides in the first lithiation process. The *in situ* produced nano-Si domains disperse uniformly in inert Li_4SiO_4/Li_2O matrix. The latter can prevent the nano-Si from electrochemical aggregation during cycling and buffer in a certain degree the big volume change caused by the lithiation of active Si, and therefore keep the geometric integrity of the electrode and improve the cycling performance. Bulk SiO_2 is generally considered as an electrochemically inactive material for lithium ion batteries due to its strong Si–O bond and low electronic conductivity. Actually, the scale and crystallinity of SiO_2 have a strong effect on its electrochemical activity. Gao et al. [26] reported that commercial SiO_2 nanoparticles with 7 nm in diameter can react with Li between 0 and 1.0 V (*vs.* Li^+/Li) with a reversible capacity of 400 mA h g^{-1}. Yao et al. [27] prepared carbon coated SiO_2 nanoparticles via a wet chemistry approach, which presented a reversible capacity of *ca.* 500 mA h g^{-1} after 50 cycles. Guo et al. [28] employed a hydrothermal method to prepare an amorphous composite of nano-SiO_2 and hard carbon (HC/SiO_2), which gives rise to a reversible capacity of *ca.* 600 mA h g^{-1} after 12 cycles.

Compared to SiO materials, the relative research on SiO_2 is very limited. Therefore, the feasibility of SiO_2 as an anode material for lithium ion batteries remains to be further investigated. In this study, a simple and productive synthesis route was employed to prepare an amorphous SiO_2/C composite anode material. The structure and electrochemical characteristics of SiO_2/C composite as an anode material were characterized. The synthesized amorphous SiO_2/C composite exhibits a high specific capacity, good cycling performance and excellent rate-capability.

2. Experimental

The SiO_2/C composite anode materials were synthesized as follows. The porous silica was synthesized by a simple sol–gel method with tetraethoxysilane (TEOS) as a starting material. Firstly, TEOS was mixed with ethanol and distilled water under vigorous stirring, and then acetic acid was added as acidic catalyst. The resulting mixture was stirred for 15 min, followed by the addition of some amount of aqueous ammonia as basic catalyst. After gelation, the gel was aged in ethanol for 3 days at ambient temperature, then the aging solution was replaced by fresh ethanol every 12 h for 4 times in order to remove the unreacted chemicals and ensure a complete solution exchange. The wet gel was then dried at room temperature for 1 day and then 80 °C for 2 days to obtain the desired porous silica. The porous silica was ball-milled with ethanol as medium using a planetary ball mill at a constant rotation speed of 400 rpm for 5 h at room temperature. A certain amount of sucrose as carbon source was added into the ball-milled slurry with vigorous stirring and then the mixture was dried by rotary evaporator and heat-treated at 900 °C under N_2 atmosphere.

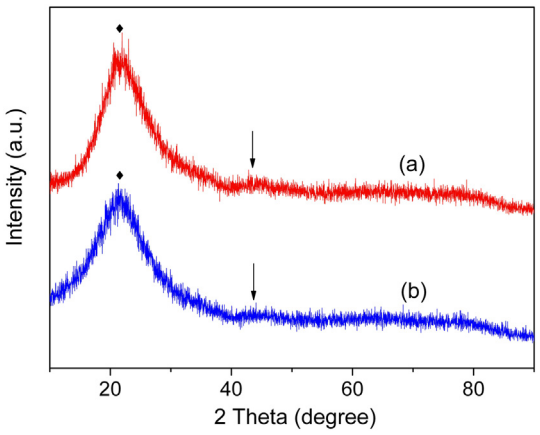

Fig. 1. XRD patterns of samples SiO_2/C-BM (a) and SiO_2/C (b).

The obtained sample is labelled as SiO_2/C-BM. For comparison, the SiO_2/C sample was synthesized following the same procedures except the porous silica was not subjected to ball milling.

The phase characterization of samples was carried out by using a powder X-ray diffraction (XRD, Rigaku, D/max-A, Cu Kα, $\lambda = 1.5406$ Å) over 2θ degree from 10° to 90°. The carbon content of the samples was determined with the LECO CS230 carbon–sulfur analyzer while the oxygen content was determined with the LECO TC600 oxygen–nitrogen analyzer. Silicon amount was calculated as a difference to 100% assuming to have less than 1 wt.% of other element in the material. The particle morphology of synthesized powders was observed by field emission scanning electron microscope (FESEM, SUPRA55) and the microstructure of the samples was identified by high resolution transmission electron microscope (HRTEM, JEM-2010).

The electrochemical performance of the as-prepared samples was evaluated using CR2032 coin cell with porous polypropylene (Celgard 2400) film as separator, lithium-foil as counter electrode, and 1 M $LiPF_6$ in a non-aqueous solution of ethylene carbonate (EC), ethylmethyl carbonate (EMC) and dimethyl carbonate (DMC) with a volume ratio of 1:1:1 as electrolyte. The cells were assembled in an argon-filled glove box. The working electrodes were prepared by mixing the active materials, acetylene black (AB) and polyvinylidene fluoride (PVDF) together at a mass ratio of 70:15:15, using *N*-methyl-2-pyrrolidone (NMP) as the solvent. The electrode slurry was spread onto a copper foil. After drying at ambient temperature and then 70°C-oven, the electrode film was pressed and cut into circular discs with a diameter of 8 mm. The discs were weighted and dried again at 120 °C for 24 h under vacuum environment for cells assemble. The charge/discharge cycle test was carried out with LAND CT2001A tester (Wuhan, China) at different current densities in the voltage range of 0.01–2.5 V versus Li^+/Li.

3. Results and discussion

The XRD patterns of the prepared samples SiO_2/C-BM and SiO_2/C are shown in Fig. 1. There are no distinct diffraction peaks for both samples, indicating the amorphous feature of the powders. A broad and weak diffraction peak located in the 2θ range of 21–23° should be associated with amorphous SiO_2 [29] and the weak peak around 43° is assignable to carbon [30]. There is no obvious difference between the two samples from XRD patterns. The element analysis reveals that both samples have similar chemical composition, the O/Si ≈ 2 and the carbon content is 7.5 wt.%.

The FESEM images of samples SiO_2/C-BM and SiO_2/C are presented in Fig. 2. As shown in Fig. 2(b), the sample SiO_2/C exhibits a

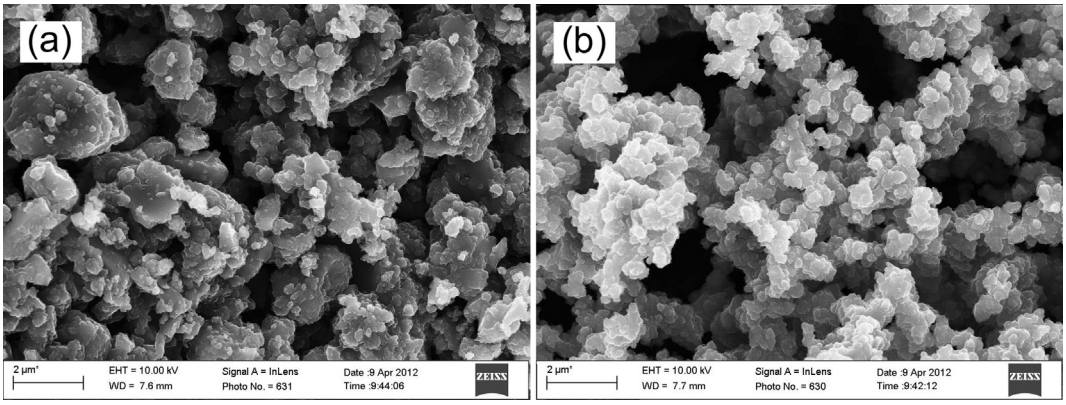

Fig. 2. FESEM images of samples SiO_2/C-BM (a) and SiO_2/C (b).

sponge-like microstructure composed of many pores and highly cross-linked network, which is similar with that of pure silica aerogel [31,32]. The apparent particle size is 200–300 nm. After ball-milling for 5 h in a planetary ball-mill, part of the particle size of silica decreases obviously (Fig. 2(a)). The small particles aggregate severely into larger particles due to surface tension. The sample SiO_2/C-BM remains porous, similar with sample SiO_2/C.

In order to gain insight into the microstructure of the SiO_2/C materials with and without ball-milling, the two samples SiO_2/C-BM and SiO_2/C were observed under HRTEM. The HRTEM images of both samples are depicted in Fig. 3. Both samples display an amorphous carbon layer coated on SiO_2 particles. For sample SiO_2/C without ball-milling, lots of nano-crystalline SiO_2 domains with size of 3–10 nm are dispersed in amorphous phase matrix, as shown in Fig. 3(b). The lattice fringes in the crystalline domains are consistent well with the lattice spaces of SiO_2 (311) and (222), as indicated in Fig. 3(b). The crystalline SiO_2 domains with different orientations connect directly or via amorphous part. For sample SiO_2/C-BM, however, the silica shows fully amorphous feature, since no lattice fringe is observed. The mechanical milling process is believed to be responsible for the amorphization [33,34].

The electrochemical performances of samples SiO_2/C-BM and SiO_2/C are plotted in Fig. 4. Compared with SiO_2/C electrode, SiO_2/C-BM electrode exhibits a higher initial discharge capacity (835.2 *vs.* 281.2 mA h g^{-1}) and charge capacity (505 *vs.* 85.9 mA h g^{-1}). Sample SiO_2/C delivers a stable but lower specific capacity of *ca.* 100 mA h g^{-1} during 50 cycles, suggesting that crystallized SiO_2 has poor electrochemical activity towards lithium ion storage. This is probably due to the strong Si–O bond of crystalline SiO_2. Meanwhile, SiO_2/C-BM electrode displays a high specific capacity and an excellent cycling stability. The charge capacity shows a slightly increase tendency at first 20 cycles and then remains at ~600 mA h g^{-1} till 100 cycles without any tendency of degradation. This indicates that amorphous SiO_2 has higher electrochemical activity than SiO_2 with crystalline cluster. The disordered structure of amorphous SiO_2 with changed bond length and bond angle has weak bond strength, which should be responsible for its high electrochemical activity as anode in lithium ion cell. The carbon layer on the SiO_2 surface can prevent the SiO_2 particle from aggregation and together with the porous feature of SiO_2 can buffer the volume change induced by the lithiation/delithiation of SiO_2 in certain extent, and thus making great contribution to the excellent cycling stability.

To evaluate the rate-capability of sample SiO_2/C-BM, the stepped cycling test was carried out at different current densities. The results are shown in Fig. 4(b). The SiO_2/C-BM electrode exhibits an excellent rate-capability. At first 10 cycles (0.1 A g^{-1}) the capacity still shows a climbing phenomenon, gradually reaching to *ca.*

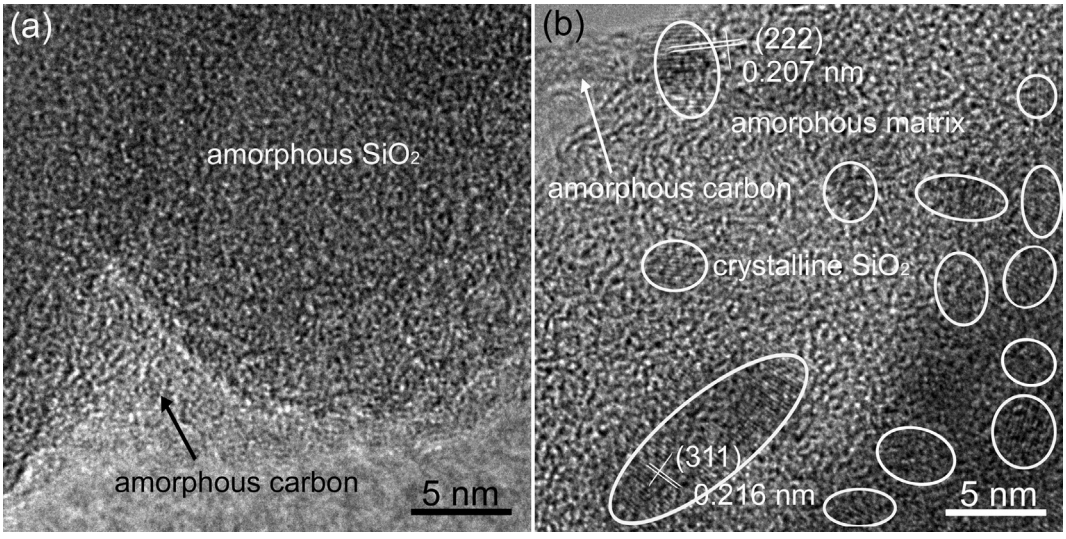

Fig. 3. HRTEM images of samples SiO_2/C-BM (a) and SiO_2/C (b).

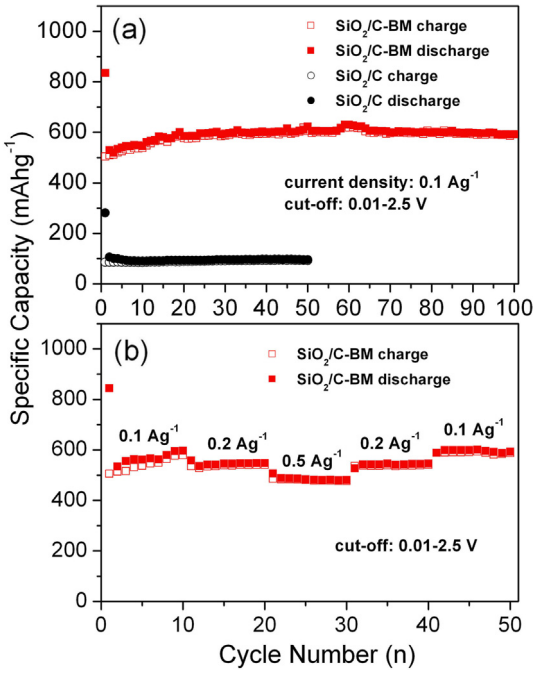

Fig. 4. (a) Cycling performance of samples SiO_2/C-BM and SiO_2/C and (b) rate-capability of sample SiO_2/C-BM.

600 mA h g^{-1}. With increasing current density, the reversible capacity decreases slightly. Even at 0.5 A g^{-1}, the SiO_2/C-BM electrode can deliver a reversible capacity of *ca.* 480 mA h g^{-1}. When the current density switches back from 0.5 to 0.1 A g^{-1}, the reversible capacity recovers to *ca.* 590 mA h g^{-1}. The electrode presents a good structural stability and excellent rate performance. This is associated with the carbon coating layer on the SiO_2 particle surface, which can provide good electronic conductivity for electrode reaction and thus improve the rate capability of electrode [3]. On the other hand, the porous structural characteristics of SiO_2/C material allow more electrolyte to be absorbed into active materials, and thus also make part contribution to the good rate-capability and cycling stability of the electrode.

4. Conclusions

Amorphous SiO_2/C composite material was synthesized via sol–gel route combining with ball-milling and post heat-treatment processes. As anode material for lithium ion batteries, the ball-milled SiO_2/C electrode shows high specific capacity (~600 mA h g^{-1}), excellent cycling stability and good rate capability. The SiO_2 with nano-crystalline domains demonstrates poor electrochemical activity, while the amorphous SiO_2 exhibits high electrochemical activity towards lithium storage. Porous silica is a good precursor for SiO_2-based anode material, which can be easily amorphized by mechanical milling. Carbon component plays important roles in stabilizing the electrode structure and improving the rate-capability of electrode. Considering the facile and productive preparation route and the good electrochemical properties, the ball-milled amorphous SiO_2/C has considerable potential for use as an alternative anode material for lithium ion batteries.

Acknowledgements

This work was financially supported by National Basic Research Program of China (2013CB934003), National Nature Science Foundation of China (21273019) and Guangdong Industry-Academy-Research Alliance (2009A090100020).

References

[1] M.S. Whittingham, MRS Bull. 33 (2008) 411–419.
[2] W. Zhang, J. Hu, Y. Guo, S. Zheng, L. Zhong, W. Song, L. Wang, Adv. Mater. 20 (2008) 1160–1165.
[3] J. Wang, H. Zhao, X. Liu, J. Wang, C. Wang, Electrochim. Acta 56 (2011) 6441–6447.
[4] Y. Yang, F. Liu, T. Li, Y. Chen, Y. Wu, M. Kong, Scripta Mater. 66 (2012) 495–498.
[5] Y.N. NuLi, J. Yang, M. Jiang, Mater. Lett. 62 (2008) 2092–2095.
[6] C. Chan, H. Peng, G. Liu, K. Mcllwrath, X. Zhang, R.A. Huggins, Y. Cui, Nat. Nanotechnol. 3 (2008) 31–35.
[7] Y. Yao, M.T. McDowell, I. Ryu, H. Wu, N. Liu, L. Hu, W.D. Nix, Y. Cui, Nano Lett. 11 (2011) 2949–2954.
[8] H. Wu, G. Zheng, N. Liu, T.J. Carney, Y. Yang, Y. Cui, Nano Lett. 12 (2012) 904–909.
[9] L. Cui, Y. Yang, C.M. Hsu, Y. Cui, Nano Lett. 9 (2009) 3370–3374.
[10] Y. Wang, J.R. Dahn, J. Electrochem. Soc. 153 (2006) A2188–A2191.
[11] H. Kim, M. Seo, M.H. Park, J. Cho, J. Angew. Chem., Int. Ed. 49 (2010) 2146–2149.
[12] K.L. Lee, J.Y. Jung, S.W. Lee, H.S. Moon, J.W. Park, J. Power Sources 129 (2004) 270–274.
[13] L. Chen, K. Wang, X. Xie, J. Xie, Electrochem. Solid-State Lett. 9 (2006) A512–A515.
[14] V. Baranchugov, E. Markevich, E. Pollak, G. Salitra, D. Aurbach, Electrochem. Commun. 9 (2007) 796–800.
[15] G. Wang, L. Sun, D.H. Bradhurst, S. Zhong, S. Dou, H. Liu, J. Alloys Compd. 306 (2000) 249–252.
[16] N. Dimov, S. Kugino, M. Yoshio, J. Power Sources 136 (2004) 108–114.
[17] Y.N. Jo, Y. Kim, J.S. Kim, J.H. Song, K.J. Kim, C.Y. Kwag, D.J. Lee, C.W. Park, Y.J. Kim, J. Power Sources 195 (2010) 6031–6036.
[18] D. Larcher, C. Mudalige, A.E. George, V. Porter, M. Gharghouri, J.R. Dahn, Solid State Ionics 122 (1999) 71–83.
[19] I.S. Kim, P.N. Kumta, J. Power Sources 136 (2004) 145–149.
[20] J. Saint, M. Morcrette, D. Larcher, L. Laffont, S. Beattie, J.P. Peres, D. Talaga, M. Couzi, J.M. Tarascon, Adv. Funct. Mater. 17 (2007) 1765–1774.
[21] Y.S. Jung, K.T. Lee, S.M. Oh, Electrochim. Acta 52 (2007) 7061–7067.
[22] G. Wang, J.H. Ahn, J. Yao, S. Bewlay, H. Liu, Electrochem. Commun. 6 (2004) 689–692.
[23] B.S. Lee, S.B. Son, K.M. Park, J.H. Seo, S.H. Lee, I.S. Choi, K.H. Oh, W.R. Yu, J. Power Sources 206 (2012) 267–273.
[24] J. Yang, B. Wang, K. Wang, Y. Lin, J. Xie, Z. Wen, Electrochem. Solid-State Lett. 6 (2003) A154–A156.
[25] T. Zhang, L. Fu, J. Gao, L. Yang, Y. Wu, H. Wu, Pure Appl. Chem. 78 (2006) 1889–1896.
[26] B. Gao, S. Sinha, L. Fleming, O. Zhou, Adv. Mater. 13 (2001) 816–819.
[27] Y. Yao, J. Zhang, L. Xue, T. Huang, A. Yu, J. Power Sources 196 (2011) 10240–10243.
[28] B. Guo, J. Shu, Z. Wang, H. Yang, L. Shi, Y. Liu, L. Chen, Electrochem. Commun. 10 (2008) 1876–1878.
[29] H. Fukui, H. Ohsuka, T. Hino, K. Kanamura, ACS Appl. Mater. Interfaces 2 (2010) 998–1008.
[30] J. Wang, H. Zhao, J. He, C. Wang, J. Wang, J. Power Sources 196 (2011) 4811–4815.
[31] L. Wang, S. Zhao, M. Yang, Mater. Chem. Phys. 113 (2009) 485–490.
[32] S.D. Bhagat, Y.H. Kim, M.J. Moon, Y.S. Ahn, J.G. Yeo, Solid State Sci. 9 (2007) 628–635.
[33] Z. Lu, L. Zhang, X. Liu, J. Power Sources 195 (2010) 4304–4307.
[34] L. Ning, Y. Wu, S. Fang, E. Rahm, R. Holze, J. Power Sources 133 (2004) 229–242.